REJUVENATION RESEARCH
Volume 18, Number 5, 2015

DOI: 10.1089/rej.2014.1651

Protective Effect of Super-Critical Carbon Dioxide Fluid Extract from Flowers and Buds of *Chrysanthemum indicum* Linnén Against Ultraviolet-Induced Photo-Aging in Mice

Xie Zhang,* You-Liang Xie,* Xiu-Ting Yu, Zu-Qing Su, Jie Yuan, Yu-Cui Li, Zi-Ren Su, Janis Ya-Xian Zhan, and Xiao-Ping Lai

Abstract

It is known that solar ultraviolet (UV) radiation to human skin causes photo-aging, including increases in skin thickness and wrinkle formation and reduction in skin elasticity. UV radiation induces damage to skin mainly by superfluous reactive oxygen species and chronic low-grade inflammation, which eventually up-regulate the expression of matrix metalloproteinases (MMPs). In this study, the super-critical carbon dioxide extract from flowers and buds of *Chrysanthemum indicum* Linnén (CI_{SCFE}), which has been reported to possess free radical scavenging and anti-inflammatory properties, was investigated for its photo-protective effect by topical application on the skin of mice. Moreover, CI_{SCFE} effectively suppressed the UV-induced increase in skin thickness and wrinkle grading in a dose-dependent manner, which was correlated with the inhibition of loss of collagen fiber content and epidermal thickening. Furthermore, we observed that CI_{SCFE} could obviously decrease UV-induced skin inflammation by inhibiting the production of inflammatory cytokines (interleukin-1β [IL-1β, IL-6, IL-10, tumor necrosis factor-α), alleviate the abnormal changes of anti-oxidative indicators (superoxide dismutase, catalase, and glutathione peroxidase), and down-regulate the levels of MMP-1 and MMP-3. The results indicated that CI_{SCFE} was a novel photo-protective agent from natural resources against UV irradiation.

Introduction

Long-term exposure to sunlight or ultraviolet (UV) radiation leads to premature aging of skin, so-called photo-aging.[1] The manifestations of photo-aged human skin, including coarse wrinkles, laxity, and uneven pigmentation, are associated with loss of elasticity and degradation of collagen in the skin organizational structure.[2,3] These abnormal alterations can be ascribable to UV radiation–induced over-production of reactive oxygen species (ROS) and multiple inflammatory cytokines.[4–6] Previous reports have confirmed that elevated generation of ROS initiates oxidative damage to DNA, proteins, and lipids in the skin, resulting in photo-damage, photo-aging, and photo-carcinogenesis.[7,8] In addition, increased ROS productions can overwhelm endogenous anti-oxidant defense systems via depleting anti-oxidative enzymes containing superoxide dismutase (SOD), glutathione peroxidase (GSH-Px), and catalase (CAT), leaving the skin vulnerable to attack from ROS.[9] In response to UV radiation–caused oxidative damage, the mitogen-activated protein kinase (MAPK) signaling transduction pathway is triggered.[3,10] Therewith, inducible nuclear factor kappa B (NF-κB) and associated protein-1 (AP-1) signaling transduction pathways are activated, stimulating the secretion of a large number of inflammatory mediators such as interleukin-1β (IL-1β), IL-6, IL-10, and tumor necrosis factor-α (TNF-α),[11] which leads to skin inflammation characterized by erythema, immunosuppression, and edema.[12] Moreover, excessive oxidative stress and inflammation responses bring about the over-expression of a series of matrix metalloproteinases (MMPs), which are responsible for photo-damaged skin.[13] Consequently, it can be concluded that an agent exerting potent anti-oxidant and anti-inflammation activities may be a promising photo-protective drug.

Chrysanthemum indicum Linnén (*C. indicum*), an oriental traditional medicine, has been used to treat inflammation, immune-related disorders, hypertension, and several infectious diseases,[14–17] with a high efficacy and minimal side-effect profile.[16] It was reported that the prominent constituents in *C. indicum*, including flavonoids, terpenoids, and phenolic compounds, could be responsible for its therapeutic properties.[18] According to a series of previous studies, we found that *C. indicum* inhibited the activation of MAPKs and

School of Chinese Materia Medica, Guangzhou University of Chinese Medicine, Guangzhou, People's Republic of China.
*These authors contributed equally to this work.

NF-κB–dependent pathways to reduce the production of inflammatory mediators, such as nitric oxide (NO), TNF-α, and IL-1β.[19] In addition, there is a growing recognition that *C. indicum* showed anti-oxidative effects attributed to excellent scavenging activity on 2,2-diphenyl-1-picrylhydrazyl (DPPH) and hydroxyl radical, thus attenuating free radical–induced DNA damage.[17]

Importantly, the super-critical carbon dioxide fluid extract from flowers and buds of *C. indicum* (CI_{SCFE}) has been applied extensively as a fine material in numerous traditional Chinese medicinal preparations (*e.g.*, *C. indicum* granules and capsules), cosmetics (*e.g.*, facial masks and creams), and toiletries (*e.g.*, toothpastes and mouth washes).[20] Our previous studies have revealed that CI_{SCFE} possessed an anti-inflammatory effect via increasing the activities of anti-oxidant enzymes (SOD and GSH-Px) and decreasing the production of NF-κB, TNF-α, IL-1, and IL-6.[20] Currently, the commercial application of CI_{SCFE} for a skin care and an anti-aging product is widely used in southwestern China. However, scientific studies about its efficacy against UV radiation–induced skin aging in *vivo* still remained rare. Therefore, in this study, we aimed to investigate the anti-aging effect of CI_{SCFE} in an experimental animal model of photo-aging by detecting various anti-oxidant and anti-inflammatory indicators.

Materials and Methods

Materials and chemicals

Lyoxyl 40 hydrogenerated castor oil (Cremophor® RH-40) was purchased from BASF-SE (Ludwigshafen, Germany). Phosphate-buffered saline (PBS) was obtained from Thermo Fisher Scientific (Beijing, China). SOD, GSH-Px, CAT, and malondialdehyde (MDA) were measured by using commercial kits from Jiancheng Institution of Biotechnology (Nanjing, China). Rat IL-10, IL-6, and TNF-α enzyme-linked immunosorbent assay (ELISA) reagents were purchased from eBioscience (San Diego, CA). Other commercially available ELISA kits used for determination of IL-1β, MMP-1, as well as MMP-3 were purchased from Wuhan Cusabio Biotechnology Co. Ltd, China. All other chemicals and reagents were of analytical grade.

Preparation of CI_{SCFE}

CI_{SCFE} was provided by the Institute of New Drug Research & Development, Guangzhou University of Chinese Medicine (Lot 20121104). The chemical compositions of CI_{SCFE} were determined by combining gas chromatography mass spectrometry (GC-MS) with high-performance liquid chromatography with photodiode array detector (HPLC-PAD) as our previous study described.[20,21] According to our previous report, 35 compounds were determined by GC-MS, and five components were identified using HPLC-PAD (the brief chemical profile of CI_{SCFE} is presented in Table S1) (Supplementary Data are available at www.liebertonline.com/rej/). In this study, the same extract was also used and CI_{SCFE} was dissolved by RH-40 to yield three different concentrations: 10 mg/mL, 30 mg/mL, and 100 mg/mL.

Grouping of animals

Sixty-three female Kunming mouse (20–22 grams) were obtained from the animal center of Guangzhou University of Chinese Medicine (GZUCM). All experimental protocols were approved by the Institutional Animal Care and Use at GZUCM. The mice were housed under conventional conditions at a controlled temperature (23 ± 2°C), humidity (55 ± 10%) and maintained under a natural light/dark cycle. Mice had free access to standard laboratory diet and water during this experiment. The experimental mice were randomized divided into seven groups and transferred to cages (nine mice per cage) (Table 1). After the mice were anesthetized using ether inhalation, the dorsal skin of the mice was shaved with a safety razor for $2.5 \times 2.5\ cm^2$.

UV irradiation and CI_{SCFE} treatment

Simulated solar irradiation was provided by an array of seven UVB lamps (285–350 nm) surrounding three UVA lamps (320–400 nm, Waldmann UV800, Germany). The mice were irradiated keeping the distance at 30 cm from UV lamps five times a week for 10 weeks. The dose gradually reached 4 minimal erythema doses (MED) by the end of the fourth week of exposure, which was measured by a UV meter (Waldmann Lichttechnik GmbH, Germany). This was accomplished by increments of 1 MED per week from 1 MED (1 MED = 70 mJ/cm^2) at week 1. Then the mice were irradiated at 4 MED for further 6 weeks.

CI_{SCFE} at different concentrations or the vehicle (120 μL/mouse) were applied topically to the shaved dorsal skin before each exposure to UV irradiation. The final doses of CI_{SCFE} were 1.2, 3.6, and 12.0 mg/ mouse, as shown in Table 1.

Evaluation of the skin visual appearance, elasticity, and thickness induced by UV irradiation

In this protocol, the appearance of skin in mice began to be observed macroscopically in the dorsal region after the initiation

Table 1. Study Treatment Schedule

Group	Shave	UV radiation	Vehicle 120 μL/mouse	CI_{SCFE} (mg/mouse)		
				1.2	3.6	12
Naïve control (NC)	−	−	−	−	−	−
Sham control (SC)	+	−	−	−	−	−
Model control (MC)	+	+	−	−	−	−
Vehicle control (VC)	+	+	+	−	−	−
CI_{SCFE} low dose (CI_{SCFE} −L)	+	+	+	+	−	−
CI_{SCFE} middle dose (CI_{SCFE}-M)	+	+	+	−	+	−

CI_{SCFE}, *C. indicum* super-critical carbon dioxide fluid extract.

of UV irradiation. Each mouse was anesthetized, and then the UV-irradiated dorsal area was photographed. Skin macroscopic visual score was estimated by blinded investigators in terms of a grading scale based on the experimental model proposed by Bisset et al.[22] To test skin elasticity, a pinch test was carried out weekly in accordance with the modified protocol described by Tsukahara et al.[23] Briefly, The dorsal skin at the midline of mice was picked up with the fingers as much as possible until its feet were just in touch with the table. After release, the time(s) until the skin recovered to the original state was measured. The skin-fold thickness after UV irradiation were measured every week using a Quick Mini Caliper (Mitutoyo Co., Kanagawa, Japan).[24]

Histopathology studies

The dorsal skin samples removed at the end of tenth week were fixed in 10% neutral-buffered formalin for 24 hr, embedded in paraffin under vacuum, and sectioned at 5-μm thickness. The degree of skin structure alteration and elastosis were assessed visually using Hematoxylin & Eosin (H&E) staining and Gomori's Aldehyde Fuchsin staining. After the same cross sections were selected from three slides per sample, five different locations (magnification, 200×) per slide were photographed. Histological alterations were evaluated and quantified through the image analysis program ImageJ 1.36 (Wayne Rasband, National Institutes of Health, Bethesda, MD).[25,26]

The determination of total collagen

The total collagen synthesis in skin tissue after UV radiation exposure was measured by total cutaneous hydroxyproline (Hyp) assay. Hyp usually can be converted to the equivalent of collagen by multiplying the factor 7.46, because Hyp is the almost exclusive amino acid of collagen and accounts for 13.4 ± 0.24 percent of mammalian collagen in previous studies.[27,28]

Determination of SOD, GSH-Px, CAT, and MDA in the skin

The freshly removed skin tissue (0.4 gram) was homogenized (10,000 rpm, 20 sec) with an Ultra-Turrax homogenizer (T18 Basic, IKA) in 9 volumes of cold normal saline (4°C). Before centrifugation, 0.15 mL of the homogenate was taken out for the MDA assay and the rest was centrifuged at $3000 \times g$ for 20 min at 4°C. The total supernatant was used for total (T)-SOD, GSH-Px, and CAT measurements according to the manufacturers' protocols.

Determination of IL-1β, IL-6, IL-10, TNF-α, MMP-1, and MMP-3 in the skin

Another skin tissue (0.4 gram) was homogenized (10,000 rpm, 20 sec) with an Ultra-Turrax homogenizer in 9 volumes of PBS (4°C) to collect the 10% homogenate. The homogenate subsequently was centrifugated at $3000 \times g$ for 20 min at 4°C. The supernatant was used to estimate the secreted IL-1βIL-6, IL-10, TNF-α, MMP-1, and MMP-3 using ELISA kits according to the manufacturer's instructions.

Statistical analysis

Experimental results are expressed as mean values ± standard error of the mean (SEM), as noted in the following figures and tables. These data were analyzed by one-way analysis of variance (ANOVA) followed by the Tukey test as a post hoc comparison for multiple pairwise comparisons, considered statistically significant at $p < 0.05$. All analysis was performed with the software Statistical Analysis Software (SPSS 17.0).

Results

Suppressive effect of CI_{SCFE} on UV radiation–induced visual skin lesions

The typical images in UV radiation–induced macroscopic skin lesions of experimental mouse at tenth week were shown in Fig. 1A. Mice in the model control (MC) and vehicle control (VC) groups presented with deep wrinkles, erythema, edema, and skin burns, which demonstrated that the photo-aging model was established successfully and the vehicle was of no use to relieve UV radiation–triggered skin destruction. However, those mice in the non-irradiated group (SC) showed no lesions but finely wrinkled skin, indicating that the shaving operation had no damage to skin. Similar skin conditions were also observed when a high dose of CI_{SCFE} (CI_{SCFE}-H) was used. In addition, a few shallow wrinkles were appeared in mice treated with a middle dose of CI_{SCFE} (CI_{SCFE}-M) after 10 weeks. In the low-dose CI_{SCFE} (CI_{SCFE}-L) group, the mice skin showed coarse wrinkles as well as slight erythema. As shown in Fig. 1A, 10 weeks of UV radiation exposure induced a significant increase in the total score (5.7 vs. 2.0 for the controls; $p < 0.01$). The visual scores of the MC group and the VC group were not different. Nevertheless, scores of CI_{SCFE}-M and CI_{SCFE}-H groups were markedly decreased compared to VC group (4.1 and 4.4 vs.5.4 for the VC group; $p < 0.05$), revealing that CI_{SCFE} could effectively prevent UV radiation–induced skin damages.

CI_{SCFE} improved the skin elasticity in the pinch test

The dorsal skin samples of various groups were photographed after being stretched for 1 sec, and the recovery time taken by the pinched skin to return to its original shape was measured weekly during the UV irradiation period (Fig. 1B). As shown in Fig. 1B, the recovery times of the mice showed no prominent difference between the MC group and VC group, but both values were significantly greater than that in the SC group. By contrast, mean value of the recovery time was obviously decreased after the mice were treated with CI_{SCFE}-M and CI_{SCFE}-H in comparison with that in the VC group, although the group of CI_{SCFE}-L did not reduce the recovery time markedly. These results did show that, when treated with CI_{SCFE} (especially 3.6 and 12 mg/mouse), the skin elasticity of the irradiated mice could be enhanced.

Efficiency of the CI_{SCFE} on reducing epidermal thickening

Epidermal thickness was examined in detail using transmission electron microscopy (Fig. 2A). The data of epidermal thickness were calculated in Fig. 2B. A significant increase was observed in both the MC group and VC group compared to the naïve control (NC) group (Fig. 2). As a follow-up to our observation in Fig. 2B, UV irradiation induced epidermal

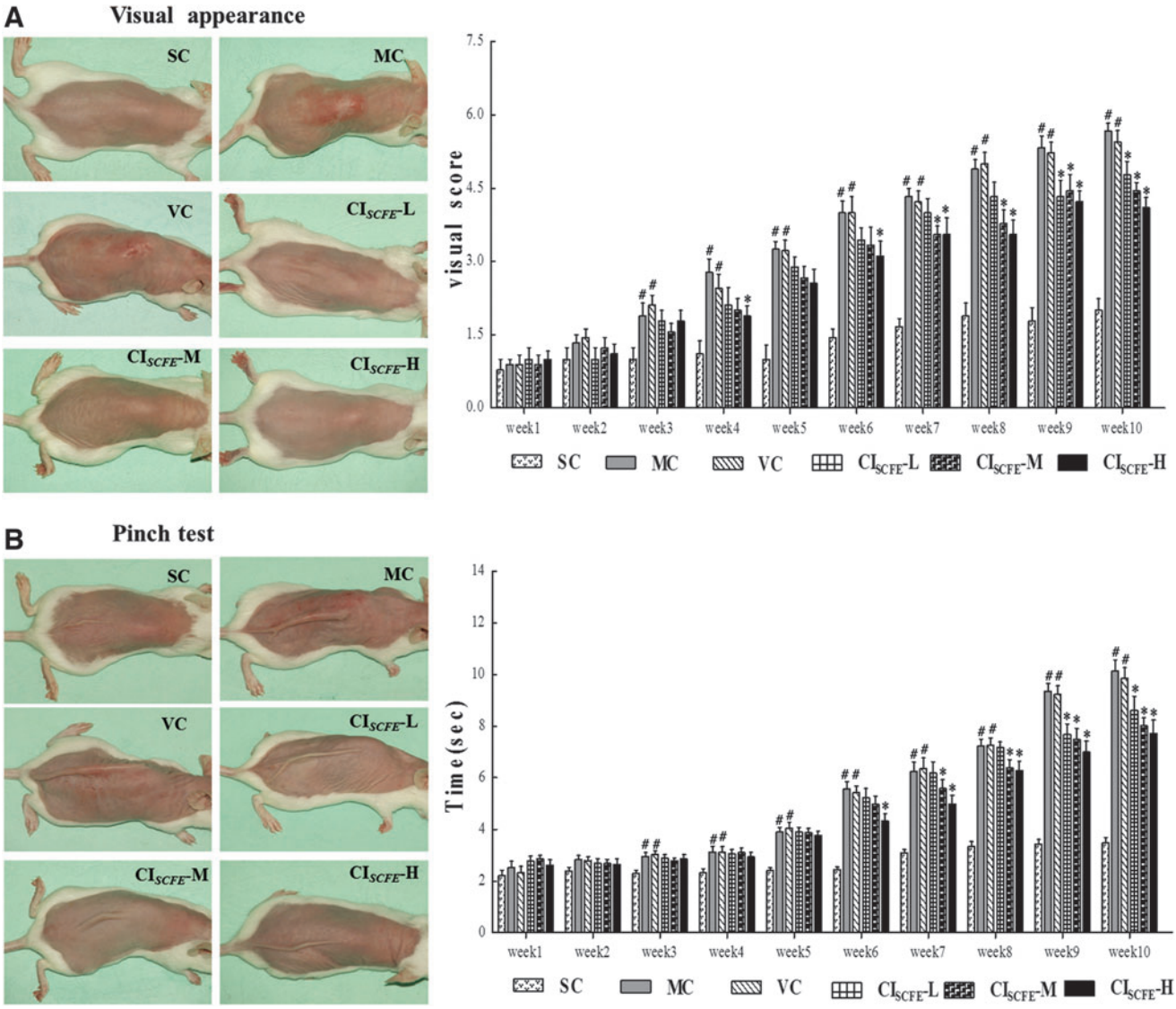

FIG. 1. Protective effect of *C. indicum* super-critical carbon dioxide fluid extract (CI_{SCFE}) on UV-induced visual skin lesions and skin elasticity in the pinch test. (**A**) Macroscopic changes and results of the visual score with different treatments at the end of study period of 10 weeks. (**B**) Pinch tests and results of the recovery time of mice in different treatment groups; the pinch test was performed according to the method described by Tsukahara. Data shown are the mean values ± standard error of the mean (SEM) ($n = 9$). (#) $p < 0.05$ compared with the SC group; (*) $p < 0.05$ compared with the VC group. SC, non-irradiated; MC, model control; VC, vehicle control; CI_{SCFE}-L low-dose CI_{SCFE}; CI_{SCFE}-M, middle-dose CI_{SCFE}; CI_{SCFE}-H, high-dose CI_{SCFE}. Color images available online at www.liebertpub.com/rej

thickening was estimated to increase to 3.4-fold as compared with the non-irradiated control skin. However, concomitant application of CI_{SCFE}-M and CI_{SCFE}-H decreased the epidermal thickening caused by UV radiation exposure by 30.94% and 41.38%. Besides, a quantitative measurement of skin fold thickness also supported the preventive effects of CI_{SCFE} on reducing skin thickness (Fig.2C).

Morphological and histological alterations of the mice skin

The anti-photo-aging effect of CI_{SCFE} was further evaluated by histological analysis of the skin specimens after routine H&E staining coupled with Gomori's Aldehyde Fuchsin staining. At the end of the 10-week period, mouse skin in NC and SC groups (Fig. 3A) showed almost similar features, displaying a complete and clear structure. The epidermis was composed of a thin stratum corneum and distinct stratum granulosum. The wavy dermal–epidermal junction (DEJ) was seen beneath the basal layer of the epidermis. The dermis is tightly connected to the epidermis through a basement membrane. As shown in Fig. 3A in the NC and SC groups, structural components of the superficial dermis were orderly arranged collagen, large amounts of elastic fibers, and extra-fibrillar matrix. Moreover, the deeper dermis also contained clusters of sebaceous gland adhered to the regular hair follicles. Inflammatory infiltrations were not observed in these two groups (Fig. 3A).

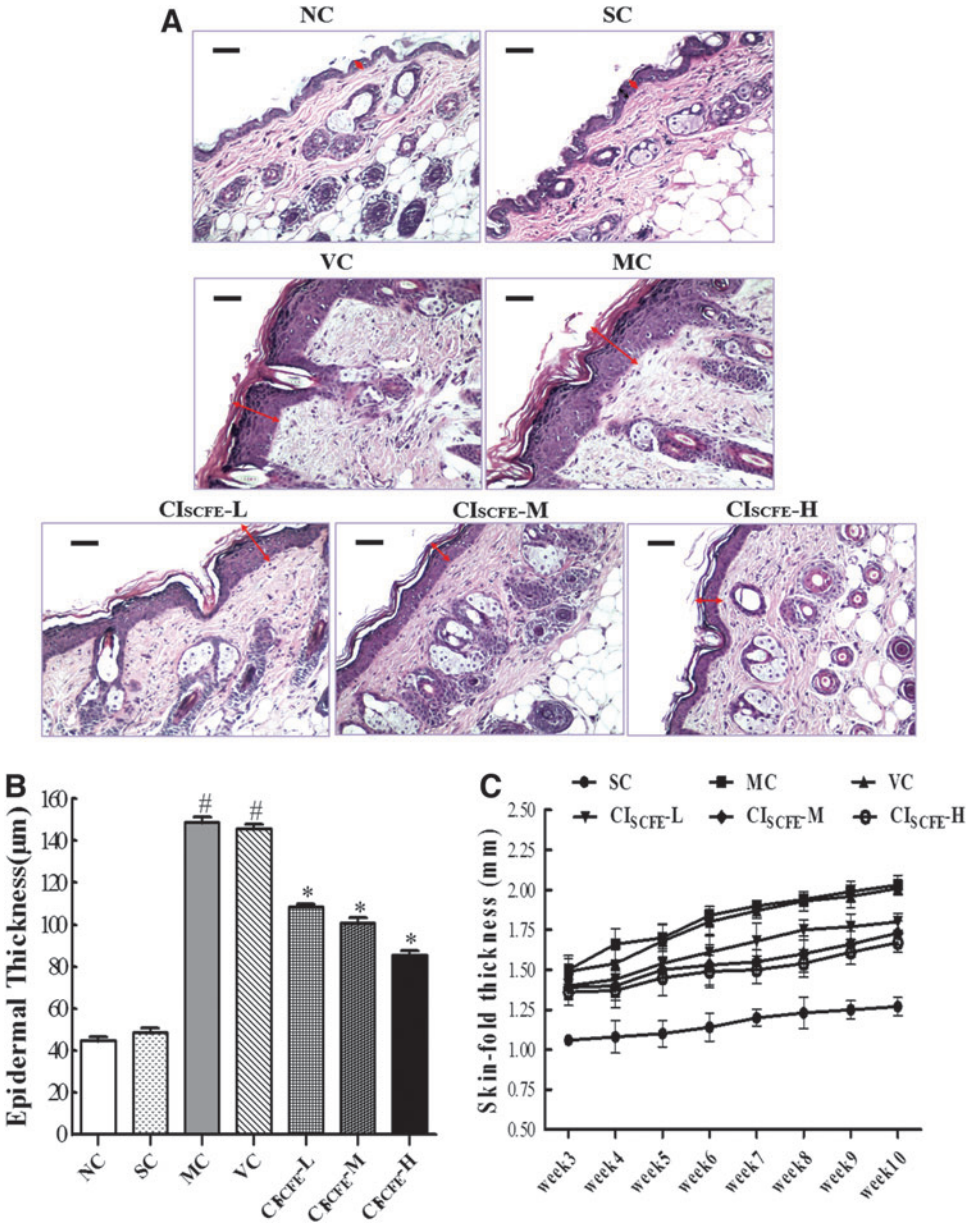

FIG. 2. Efficiency of the *C. indicum* super-critical carbon dioxide fluid extract (CI_{SCFE}) in reducing epidermal thickening. (**A**) Photographs of epidermal thickness based on Hematoxylin & Eosin (H&E) staining (original magnification, 200×). Epidermal thickness was observed by the double-headed black arrows. (**B**) Results of mean epidermal thickness of different groups. (**C**) Changes in skin fold thickness (SFT) of different groups. SFT was measured from week 3 to week 10 using a Quick Mini Caliper. Data are expressed as mean values ± standard error of the mean (SEM) of nine mice in each group. (#) $p < 0.05$ compared with the SC group; (*) $p < 0.05$ compared with the VC group. NC, naïve control; SC, non-irradiated; MC, model control; VC, vehicle control; CI_{SCFE}-L low-dose CI_{SCFE}; CI_{SCFE}-M, middle-dose CI_{SCFE}; CI_{SCFE}-H, high-dose CI_{SCFE}. Color images available online at www.liebertpub.com/rej

The histopathological features of the MC and VC groups were rather similar (Fig. 3A). UV radiation to cause skin tissue changes, including thickened stratum corneum, epidermis, and flattened DEJ, were found in the skin of group MC and VC mice. Meanwhile, there was a flattening of the rete ridges beneath the epidermis, which is believed to make the skin fragile and cause loss of nutrients. Particularly, the dermal collagen fibers were degraded, sparse, and disorganized. At the same time, the elastic fibers were reduced, tortuous, and even fractured (MC and VC groups in Fig. 4). Furthermore, dense inflammatory infiltrations as well as hemorrhage were evident in the UV radiation–exposed skin specimen.

In the CI_{SCFE}-L group, there were some similar features with the MC or VC group, but a more regular dermal collagen and elastic fibers were distributed compared to the MC mice (Fig. 3A and Fig. 4). As shown in Fig. 3A, when CI_{SCFE} (3.6 or 12 mg/mouse) was applied topically, UV radiation–induced skin structure damage was apparently

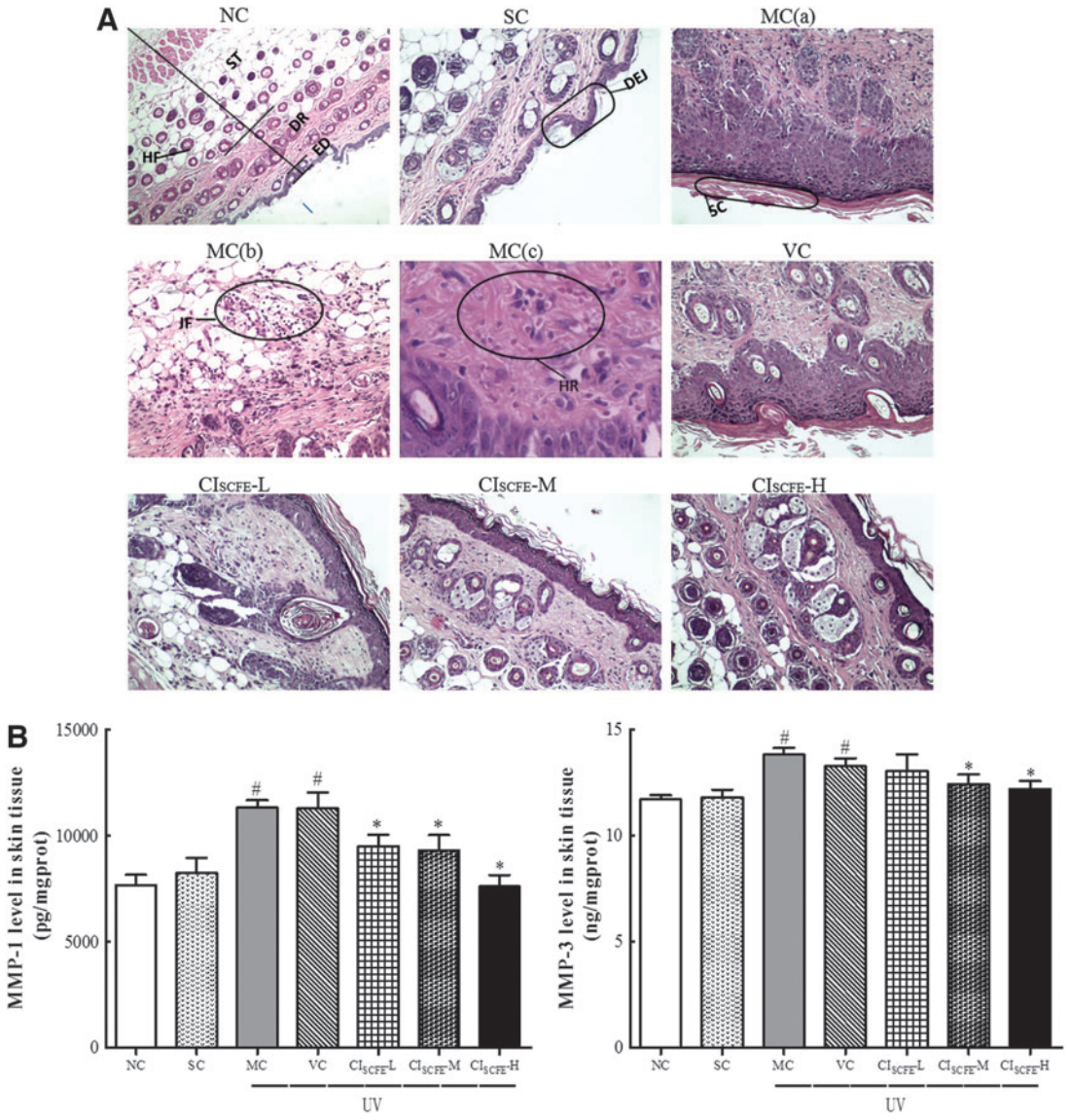

FIG. 3. Representative photographs of Hematoxylin & Eosin (H&E) staining for routine examination of the skin tissue and the effect of *C. indicum* super-critical carbon dioxide fluid extract (CI_{SCFE}) on the expression of matrix metalloproteinase-1 (MMP-1) and MMP-3. (**A**) Histological Images of mice skin based on H&E staining. NC group (magnification, 100×), representing a normal and clear structure; SC group (magnification, 100×), showing almost similar features with that in the in the NC group (magnification, 200×); MC group: (a) an abnormal structure (magnification, 200×); (b) inflammation cell gathering in and underneath the dermis (magnification, 200×); (c) disorganized and even fractured collagen bundles with hemorrhage (magnification, 400×); VC group, having similar characteristics of MC group (magnification, 200×); CI_{SCFE}-L group (magnification, 200×); CI_{SCFE}-M (magnification, 200×); CI_{SCFE}-H group (magnification, 200×). ED, epidermis; DR, dermis; ST, subcutaneous tissue; HF, hair follicle; DEJ, dermal-epidermal junction; SC, stratum corneum; IF, inflammation infiltration; HR, hemorrhage. (**B**) Results of the MMP-1 and MMP-3 expression in experimental groups. Data shown are the mean values ± standard error of the mean (SEM) ($n = 9$). (#) $p < 0.05$ compared with the SC group; (*) $p < 0.05$ compared with the VC group. NC, naïve control; SC, non-irradiated; MC, model control; VC, vehicle control; CI_{SCFE}-L low-dose CI_{SCFE}; CI_{SCFE}-M, middle-dose CI_{SCFE}; CI_{SCFE}-H, high-dose CI_{SCFE}. Color images available online at www.liebertpub.com/rej

ameliorated. First, the marked decrease in epidermal thickness as well as the curving dermal ridges were found; second, an ordered arrangement of abundant collagen bundles was displayed and the elastic fibers presented as normal in nature; finally, inflammatory infiltration and hemorrhage were absent in and underneath the fatty dermis. As a whole, there was an inhibitory effect of CI_{SCFE} on UV radiation–induced morphological and histological alterations in mice.

CI_{SCFE} inhibited the decrease of collagen content in photo-aged mice

Collagen is a main structural element in the skin that could provide support and strength.[29] Figure 5 shows that similar amounts of collagen content were detected in the NC and SC groups, whereas the collagen in the VC and MC groups was decreased compared with that in the NC and SC

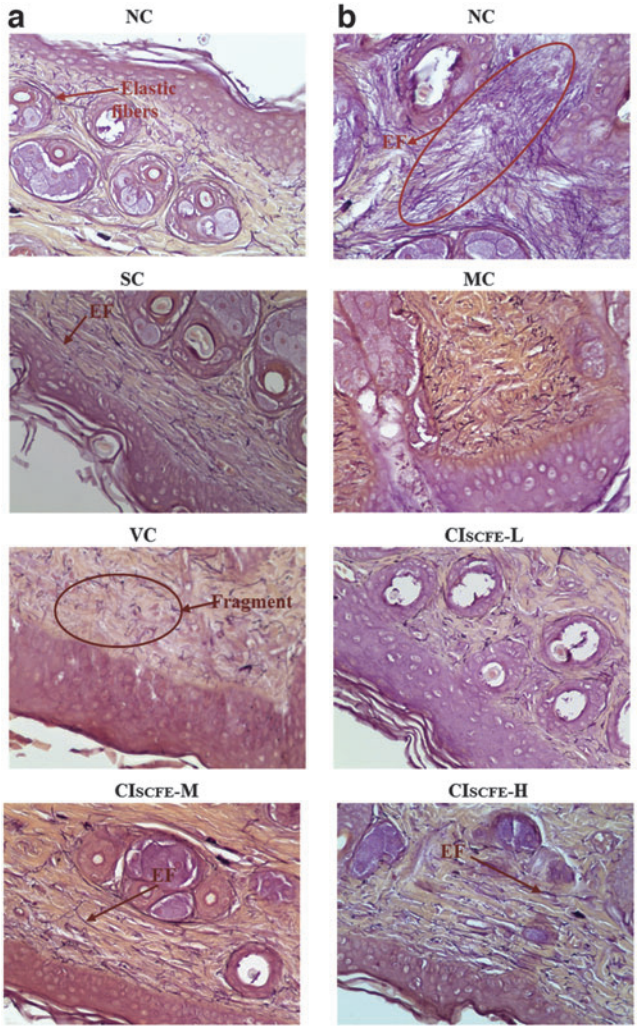

FIG. 4. Gomori's Aldehyde Fuchsin staining of back skin from experimental mice (magnification, 400×). NC group, exhibiting large amounts of organized elastic fibers; SC group, resembling the similar characteristics of NC group; MC and VC groups, showing abnormal, tangled and degraded elastic fibers. EF, elastic fibers; NC, naïve control; SC, non-irradiated; MC, model control; VC, vehicle control; CI_{SCFE}-L low-dose CI_{SCFE}; CI_{SCFE}-M, middle-dose CI_{SCFE}; CI_{SCFE}-H, high-dose CI_{SCFE}. Color images available online at www.liebertpub.com/rej

groups. In the CI_{SCFE}-L group, the mean value of collagen production was close to that in VC group. For the CI_{SCFE}-M and CI_{SCFE}-H groups, the collagen contents were statistically elevated by 33.3% and 50.1%, respectively, as compared with the VC group ($p < 0.05$). These results proved that UV radiation led to an obvious decrease in collagen content, whereas the reduction of collagen was significantly suppressed by pre-treatment of CI_{SCFE}.

Decrease in oxidative stress status through the administration of CI_{SCFE}

As depicted in Fig. 5, exposure to UV radiation induced suppression of the release of anti-oxidant enzyme production. Additionally, the levels of SOD, GSH-Px, and CAT did not differ between the NC group and the SC group, whereas the levels were significantly lowered after UV irradiation in the MC and VC group. Interestingly, the treatment with CI_{SCFE}-H and CI_{SCFE}-M could effectively reverse the reduction of GSH-Px, CAT, and SOD. These anti-oxidant enzyme contents in the CI_{SCFE}-H group were increased by 19.1%, 38.7%, and 54.2%, compared to that in the VC mice, respectively. However, there was only a slight augmentation in these enzyme contents in the CI_{SCFE}-L mice. These results indicated that CI_{SCFE} improved the activities of SOD, GSH-Px, and CAT to suppress oxidative stress following 10 weeks of chronic UV radiation exposure.

CI_{SCFE} inhibited skin MDA production

MDA is considered to be one of the most widely used indexes to reflect lipid peroxidation. As shown in Fig. 5, lipid content in MC and VC mice was significantly increased by 83.2% and 79.5%, compared to that in NC mice ($p < 0.05$). Meanwhile, no significant difference in the level of MDA was observed between NC and SC mice or MC and VC mice skin. Treatment with CI_{SCFE}-L had no apparent influence on the MDA level in the skin. In contrast, treatment with CI_{SCFE} (3.6 and 12 mg/mouse) resulted in suppression of MDA production to 0.66% and 0.63% in comparison with the VC mice, respectively. Therefore, CI_{SCFE} alleviated lipid peroxidation as a result of UV radiation damage in mice skin tissues, and the effects of CI_{SCFE}-M and CI_{SCFE}-H were much better than CI_{SCFE}-L.

The effect of CI_{SCFE} on the production of inflammatory cytokines

The production of inflammatory cytokines (IL-1β, IL-6, IL-10, TNF-α) were quantified by ELISA (Fig. 6). In general, the levels of these cytokines in the VC group were elevated significantly when compared with that in the SC group, in which IL-1β was increased by 1.40-fold, IL-6 by 1.41-fold, IL-10 by 1.60-fold, and TNF-α by 1.34-fold. However, in CI_{SCFE}-H group, these levels were highly decreased to approximately 75.5%, 80.9%, 73.6%, and 76.4% compared to that in VC group. The application with CI_{SCFE}-L did not show significant inhibition. These data provided evidence that CI_{SCFE} (especially 12 mg/mouse) could effectively inhibit the release of the inflammatory cytokines induced by UV radiation exposure.

CI_{SCFE} prevented the increase of MMP content from UV radiation–induced damage

To determine whether CI_{SCFE} inhibited UV radiation–induced MMPs expression, MMP-1 and MMP-3 expression was measured after 10 weeks irradiation. Figure 3B shows that excessive UV radiation exposure of skin distinctly elevated MMP-1 and MMP-3 content by 1.37-fold and 1.12-fold, respectively, than that in the SC mice. CI_{SCFE} significantly prevented the increase of MMP-1 in a dose-dependent manner. Meanwhile, CI_{SCFE}-M and CI_{SCFE}-H also dramatically reduced MMP-3 content in skin tissues ($p < 0.05$, vs. VC group). However, the mean content of MMP-3 in the CI_{SCFE}-L group was no longer significant when compared to that in the VC group. Overall, these data supported the preventive effect of CI_{SCFE} on UV radiation–induced MMP expression.

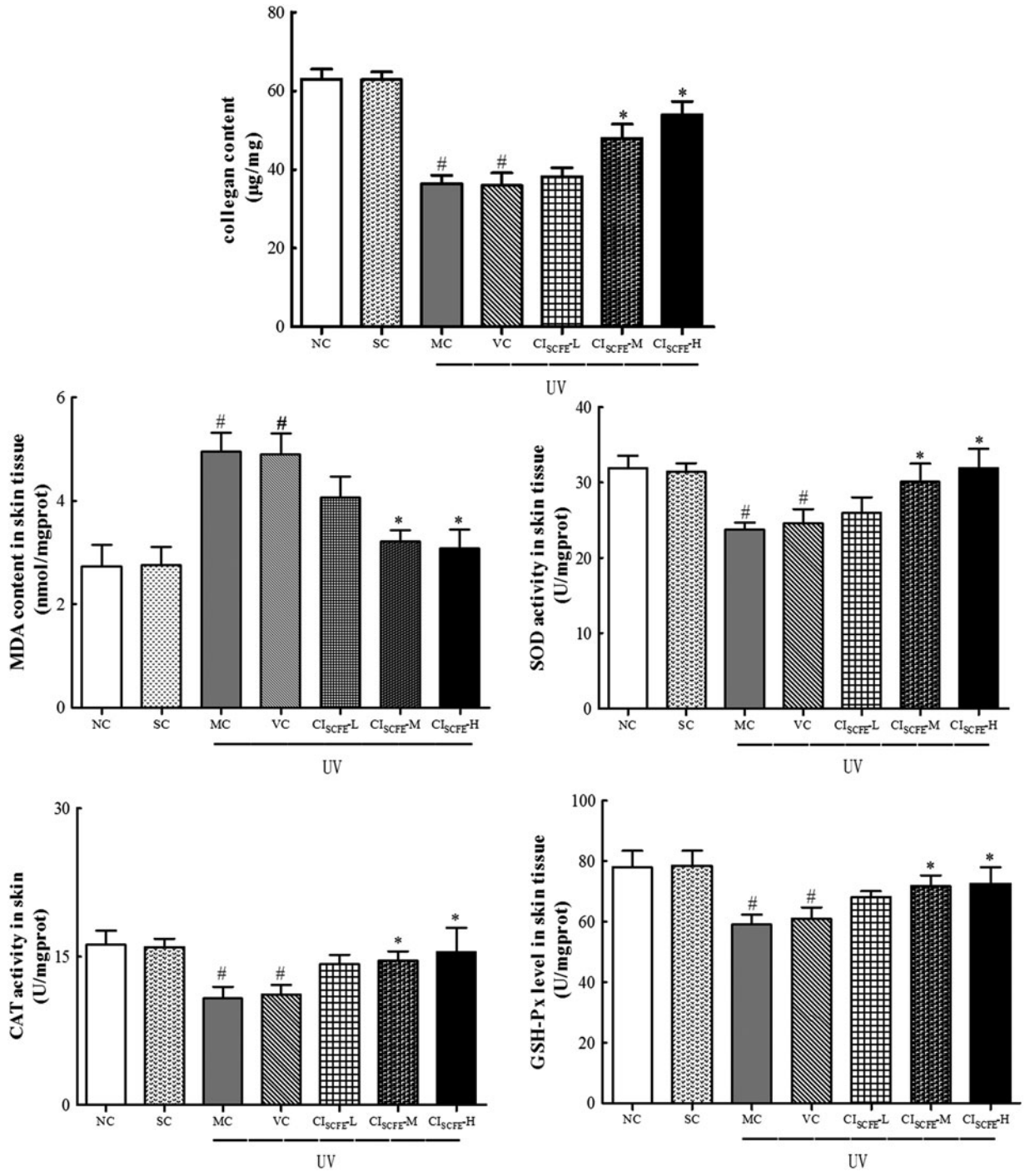

FIG. 5. Effect of *C. indicum* super-critical carbon dioxide fluid extract (CI_{SCFE}) on the activities of anti-oxidant enzymes and the levels of malondialdehyde (MDA) in photo-aged mice skin. Data are shown as mean values ± standard error of the mean (SEM) of nine mice in each group. (#) $p < 0.05$ compared to the SC group; (*) $p < 0.05$ compared to the VC group. NC, naïve control; SC, non-irradiated; MC, model control; VC, vehicle control; CI_{SCFE}-L low-dose CI_{SCFE}; CI_{SCFE}-M, middle-dose CI_{SCFE}; CI_{SCFE}-H, high-dose CI_{SCFE}.

Discussion

UV irradiation responses have been revealed to cause premature skin aging (photo-aging), which is photo-damage superimposed on the aging process, characterized by sagging, wrinkling, coarseness, and erythema.[2,30] The photo-aged skin, through the findings in previous studies, might be attributed to increased MMPs production as a result of UV radiation–induced ROS and the resulting accumulation of inflammation cytokines.[3] Currently, it has been widely proved that naturally occurring products exert protective photo-aging activity. CI_{SCFE}, a well-known agent bearing obvious anti-oxidant and anti-inflammatory activities, may be a promising effective therapeutic natural material to protect skin against photo-

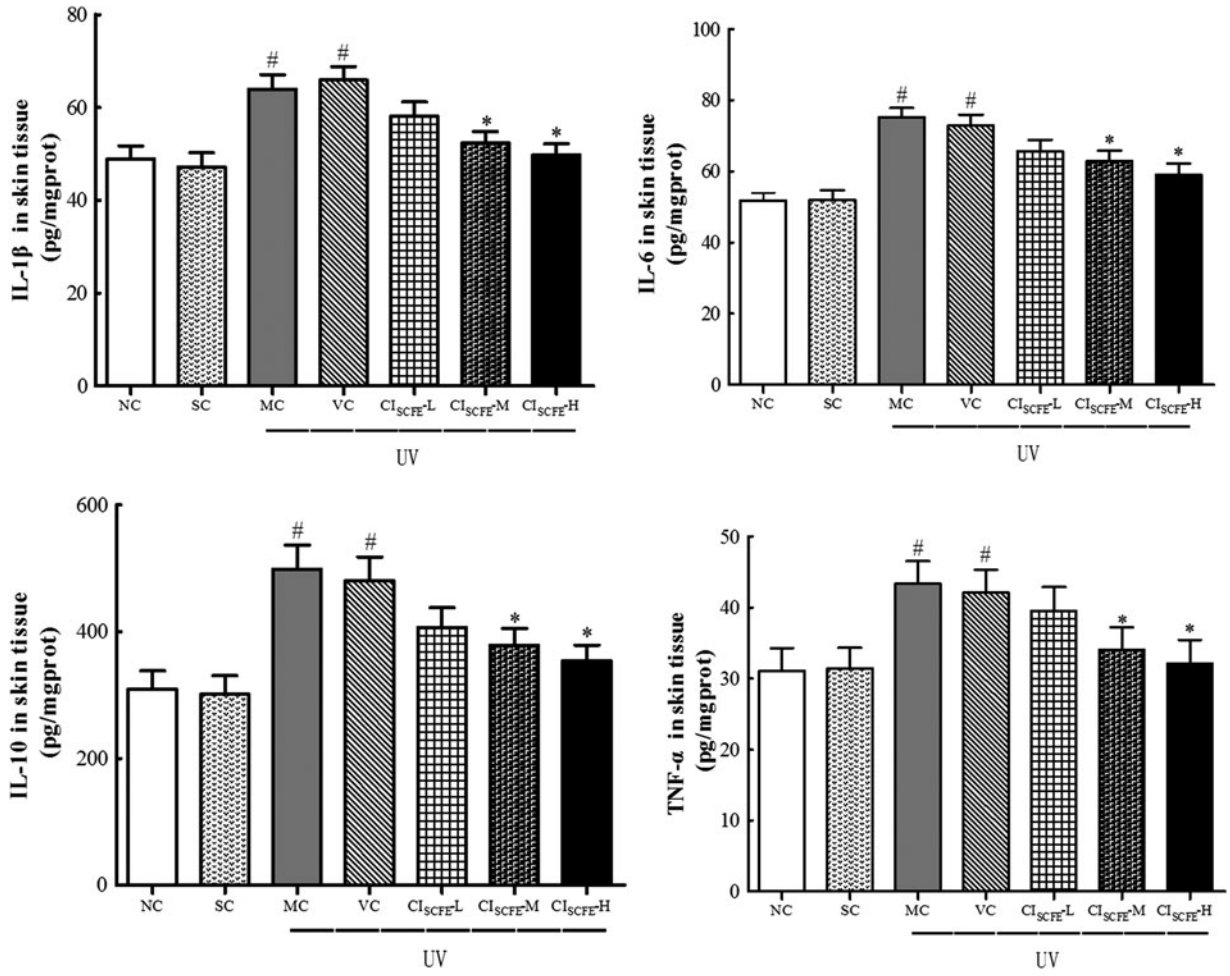

FIG. 6. Effect of *C. indicum* super-critical carbon dioxide fluid extract (CI_{SCFE}) on the expression of inflammation cytokines. Data are expressed as mean values ± standard error of the mean (SEM) of nine mice in each group. (#) $p < 0.05$ compared to the SC group; (*) $p < 0.05$ compared to the VC group. NC, naïve control; SC, non-irradiated; MC, model control; VC, vehicle control; CI_{SCFE}-L low-dose CI_{SCFE}; CI_{SCFE}-M, middle-dose CI_{SCFE}; CI_{SCFE}-H, high-dose CI_{SCFE}.

aging.[16] In this study, we investigated the anti-photo-aging property of CI_{SCFE}.

As shown in Fig. 1, chronic exposure of the skin to UV radiation caused increases in wrinkle formation and skin thickness and the reduction of skin elasticity, which is closely accordance with the decreased total collagen levels and evident elastosis in the upper dermis. These data were consistent with the previous reports.[31,32] However, in comparison with the VC group, the treatment of CI_{SCFE} inhibited the formation of wrinkles, the appearance of laxity and leathery epidermal thickening in the skin. Moreover, CI_{SCFE} (especially CI_{SCFE}-M and CI_{SCFE}-H) not only markedly prevented UV radiation–induced collagen reduction by increasing Hyp content, but also repaired the integrity of collagen structure and the elastic fibers. These findings suggested that CI_{SCFE} prevented mice skin from wrinkles and laxity, mainly by fixing collagen and elastic fibers and enhancing the collagen synthesis.

Fibrillar collagens and elastic fibers are two major constituents of dermal extracellular matrix (ECM) in connective skin tissues. The functional properties of the skin are highly dependent on collagen and elastic fiber integrity to confer tensile strength and resilience.[33] However, various UVB-induced MMPs (such as MMP-1 and MMP-3) in dermal fibroblasts are responsible for the breakdown of dermal interstitial collagen and other connective tissue components, and therefore lead to cutaneous photo-aging.[34] Thus, MMPs inhibition has been used to prevent UV radiation–induced photo-damage photo-aging.[35] In this study, we found that the topical treatment of CI_{SCFE} suppressed the increase of MMP-1 and MMP-3 expression caused by chronic UV irradiation, and this was correlated with the inhibition of the degraded elastic fibers and reduced collagen density. This result indicated that the reduction of MMPs might contribute to remodeling of ECM structures in the tissue treated with CI_{SCFE}.

Additionally, several investigations have described that up-regulation of MMPs resulted from UV radiation–induced ROS and inflammation responses.[3] Excessive ROS stimulate membrane-dependent MAPK signaling pathways and activate c-Jun and c-Fos (AP-1 protein), thus resulting in the increased MMP expression.[36] In a healthy condition, the production of ROS is constantly balanced by the anti-oxidant defense system. But if the excessive increase of ROS was induced by UV irradiation in mice skin, the defense of the endogenous anti-oxidant enzymes (SOD, CAT, and GSH-Px) is overwhelmed and then the oxidative stress

occurs.[9] Oxidative stress could cause oxidative damage to cellular components, aggravate MMPs expression and lipid peroxidation, and finally lead to skin pathologies.[37] Therefore, the removal of ROS is one of the strategies to protect skin from solar UV irradiation. In this study, topic application of CI_{SCFE} could prevent the decrease in the activities of SOD, CAT, and GSH-Px and attenuate the augmentation of MDA content in tissue, which is generally used as a reliable laboratory biomarker to evaluate the level of lipid peroxidation. This leads to inhibition of MMP-1 and MMP-3 levels and prevention of ECM degradation. Similar to our observation, Sun et al. revealed that aqueous extracts from C. *indicum* reduced photo-aging–related MMPs and strongly attenuated the elevated ROS level by UV irradiation.[38] These results revealed that the anti-photo-aging property of CI_{SCFE} was due to its protective effects on anti-oxidant enzymes, by which the ROS level could be decreased.

UV-induced erythema, edema, epidermal hyperplasia, and the production of inflammatory mediators are thought to be inflammatory responses.[39] Inflammation induced by UV irradiation plays a vital part in the development of skin photo-aging by up-regulating the expression of MMPs and damaging the cellular and molecular integrity of the dermis and the epidermis through pro-inflammatory cytokines.[40] Studies have suggested that UV radiation–induced ROS production could activate AP-1 and NF-κB to induce the production of pro-inflammatory cytokines in the skin tissue.[11] Accordingly, inhibition of UV-induced inflammatory responses is important to protect skin from photo-aging. As depicted in Fig. 1 and Fig. 3, we captured an intense inflammatory infiltrate in the photo-aged skin specimen. However, our findings showed that the levels of these cytokines (IL-1β, IL-6, IL-10, and TNF-α) were markedly reduced when treated with CI_{SCFE}. Histological results also revealed that a concentration of inflammatory cells was absent in the CI_{SCFE}-M and CI_{SCFE}-H groups, which was proved by the satiny skin shown in Fig. 1. Therefore, we concluded that CI_{SCFE} may have a photo-protective effect on the basis of its significant anti-inflammatory activity via inhibiting the excessive inflammatory cytokine production by UV irradiation.

Furthermore, with respect to chemical study of CI_{SCFE}, we hypothesized the anti-photo-aging activity of CI_{SCFE} in the present study could be due to the bioactivities of its chemical compounds. Our previous study showed that d-camphor, caryophyllene oxide, endoborneol, β-caryophyllene, eucalyptol, thymol, and bornyl acetate were the principal components of CI_{SCFE} according to the GC-MS analysis.[18] Among them, eucalyptol, thymol, d-camphor, and endoborneol were reported to effectively decrease inflammatory response in a dose-dependent manner via inhibiting pro-inflammatory mediators such as TNF-α, IL-1β, and IL-6.[41,42] By HPLC-PAD analysis, we quantified five components—chlorogenic acid, luteolin-7-glucoside, linarin, luteolin, and acacetin.[18] Wen and Chiu et al. have suggested that chlorogenic acid (phenolic acid) in *Ixora parviflora* was the major contributor to the anti-oxidant activity and it could be applied to ameliorate the incidence of photo-aging owing to significantly decreased ROS generation in UV radiation–exposed fibroblasts.[43] It was demonstrated that flavonoids (luteolin-7-glucoside, linarin, luteolin, and acacetin) have marked anti-inflammatory activity by suppressing NF-κB and MAPKs activation.[14,17,39] In addition, previous studies have revealed moderate inhibitory activities of luteolin against UVA-triggered MMP-1 production by interfering with MAPKs and AP-1 signaling.[44] Hence, compounds of CI_{SCFE}, which possess potential anti-oxidant and anti-inflammatory effects, are crucial for CI_{SCFE}'s anti-photo-aging effect, and the specific chemical compounds responsible for anti-photo-aging effect of CI_{SCFE} need to be further identified.

Summarizing, this is the first time that the anti-photo-aging effects of CI_{SCFE} have been established in an animal model, and the inhibition was ascribed to elevated collagen production via the down-regulation of MMPs, which may be mediated by the inhibition of anti-oxidant enzymes activities and inflammatory protein expression. However, further investigation is warranted for the specific chemical compounds answering for anti-photo-aging effect of CI_{SCFE} and more studies particularly related to the signaling pathways are needed to clarify the underlying mechanism of CI_{SCFE} on anti-photo-aging.

Acknowledgments

This work was supported by grants from National Natural Science Foundation of China (grant no. 81403169), Science and Technology Planning Project of Guangdong Province, China (grant nos. 2011BA101B01, 2012B030900012, 013B090600007, and 2014A020221050), the China Postdoctoral Science Foundation (grant nos. 2014M552188 and 2015T80901), the Special Funds from Central Finance of China in Support of the Development of Local Colleges and University (grant no. 276 (2014), and the Guangdong Province Universities and Colleges Pearl River Scholar Funded Scheme (2011).

Author Disclosure Statement

No competing financial interests exist.

References

1. Serafini MR, Detoni CB, Menezes Pdos P, Pereira Filho RN, Fortes VS, Vieira MJ, Guterres SS, Cavalcanti de Albuquerque Junior RL, Araujo AA. UVA-UVB photoprotective activity of topical formulations containing *Morinda citrifolia* extract. Biomed Res Int 2014;2014:587819.
2. Chung JH. Photoaging in Asians. Photodermatol Photoimmunol Photomed 2003;19:109–121.
3. Pillai S, Oresajo C, Hayward J. Ultraviolet radiation and skin aging: Roles of reactive oxygen species, inflammation and protease activation, and strategies for prevention of inflammation-induced matrix degradation—a review. Int J Cosmet Sci 2005;27:17–34.
4. Masaki H. Role of antioxidants in the skin: Anti-aging effects. J Dermatol Sci 2010;58:85–90.
5. Kondo S. The roles of cytokines in photoaging. J Dermatol Sci 2000; 23(Suppl 1):S30–S36.
6. Shah H, Mahajan SR. Screening of topical gel containing lycopene and dexamethasone against UV radiation induced photoaging in mice. Biomed Aging Pathol 2014;4:303–308.
7. Halliday GM. Inflammation, gene mutation and photoimmunosuppression in response to UVR-induced oxidative damage contributes to photocarcinogenesis. Mutat Res 2005;571:107–120.

8. Perez-Sanchez A, Barrajon-Catalan E, Caturla N, Castillo J, Benavente-Garcia O, Alcaraz M, Micol V. Protective effects of citrus and rosemary extracts on UV-induced damage in skin cell model and human volunteers. J Photochem Photobiol B 2014;136:12–18.
9. Podda M, Traber MG, Weber C, Yan LJ, Packer L. UV--irradiation depletes antioxidants and causes oxidative damage in a model of human skin. Free Radic Biol Med 1998;24: 55–65.
10. Sharma SD, Meeran SM, Katiyar SK. Dietary grape seed proanthocyanidins inhibit UVB-induced oxidative stress and activation of mitogen-activated protein kinases and nuclear factor-kappaB signaling in in vivo SKH-1 hairless mice. Mol Cancer Ther 2007;6:995–1005.
11. Djavaheri-Mergny M, Mergny JL, Bertrand F, Santus R, Maziere C, Dubertret L, Maziere JC. Ultraviolet-A induces activation of AP-1 in cultured human keratinocytes. FEBS Lett 1996;384:92–96.
12. Gibbs NK, Norval M. Photoimmunosuppression: A brief overview. Photodermatol Photoimmunol Photomed 2013;29: 57–64.
13. Fisher GJ, Voorhees JJ. Molecular mechanisms of photoaging and its prevention by retinoic acid: Ultraviolet irradiation induces MAP kinase signal transduction cascades that induce Ap-1-regulated matrix metalloproteinases that degrade human skin in vivo. J Investig Dermatol Symp Proc 1998;3:61–68.
14. Zhang JY, Zhang L, Jin Y, Cheng WM, Guo L, Zou YH, Peng L, Zhang Q, Li J. The anti-inflammatory effects of total flavonoids of chrysanthemum indicum and its partial mechanism. Acta Universitis Medicinalis Nahui 2005;5:004.
15. Zhu SY, Yang Y, Yu HD, Yu Y, Zou GL. Chemical composition and antimicrobial activity of the essential oils of *Chrysanthemum indicum*. J Ethnopharmacol 2005;96: 151–158.
16. Cheng W, Li J, You T, Hu C. Anti-inflammatory and immunomodulatory activities of the extracts from the inflorescence of *Chrysanthemum indicum* Linne. J Ethnopharmacol 2005;101: 334–337.
17. Debnath T, Jin HL, Hasnat MA, Kim Y, Samad NB, Park PJ, Lim BO. Antioxidant potential and oxidative dna damage preventive activity of chrysanthemum indicum extracts. J Food Biochem 2013;37:440–448.
18. Yoshikawa M, Morikawa T, Toguchida I, Harima S, Matsuda H. Medicinal flowers. II. Inhibitors of nitric oxide production and absolute stereostructures of five new germacrane-type sesquiterpenes, kikkanols D, D monoacetate, E, F, and F monoacetate from the flowers of *Chrysanthemum indicum* L. Chem Pharmaceut Bull Tokyo 2000;48:651–656.
19. Cheon MS, Yoon T, Lee do Y, Choi G, Moon BC, Lee AY, Choo BK, Kim HK. *Chrysanthemum indicum* Linne extract inhibits the inflammatory response by suppressing NF-kappaB and MAPKs activation in lipopolysaccharide-induced RAW 264.7 macrophages. J Ethnopharmacol 2009;122:473–477.
20. Wu XL, Li CW, Chen HM, Su ZQ, Zhao XN, Chen JN, Lai XP, Zhang XJ,Su ZR. Anti-inflammatory effect of supercritical-carbon dioxide fluid extract from flowers and buds of *Chrysanthemum indicum* Linnen. Evid Based Complement Alternat Med 2013;2013:413237.
21. Wu XL, Feng XX, Li CW, Zhang XJ, Chen ZW, Chen JN, Lai XP, Zhang SX, Li YC, Su ZR. The protective effects of the supercritical-carbon dioxide fluid extract of *Chrysanthemum indicum* against lipopolysaccharide-induced acute lung injury in mice via modulating Toll-like receptor 4 signaling pathway. Mediators Inflamm 2014;2014:246407.
22. Bissett DL, Hannon DP, Orr TV. An animal model of solar-aged skin: Histological, physical, and visible changes in UV-irradiated hairless mouse skin. Photochem Photobiol 1987;46:367–378.
23. Tsukahara K, Moriwaki S, Hotta M, Fujimura T, Sugiyama-Nakagiri Y, Sugawara S, Kitahara T, Takema Y. The effect of sunscreen on skin elastase activity induced by ultraviolet-A irradiation. Biol Pharmaceut Bull 2005;28: 2302–2307.
24. Ibbotson SH, Moran MN, Nash JF, Kochevar IE. The effects of radicals compared with UVB as initiating species for the induction of chronic cutaneous photodamage. J Invest Dermatol 1999;112:933–938.
25. Wu YY, Tian Q, Li LH, Khan MN, Yang XQ, Zhang ZM, Hu X, Chen SJ. Inhibitory effect of antioxidant peptides derived from *Pinctada fucata* protein on ultraviolet-induced photoaging in mice. J Funct Foods 2013;5; 527–538.
26. Bernstein EF, Lee J, Brown DB, Yu R, Van Scott E. Glycolic acid treatment increases type I collagen mRNA and hyaluronic acid content of human skin. Dermatol Surg 2001;27:429–433.
27. Kong SZ, Shi XG, Feng XX, Li WJ, Liu WH, Chen ZW, Xie JH, Lai XP, Zhang SX, Zhang XJ. Inhibitory effect of hydroxysafflor yellow a on mouse skin photoaging induced by ultraviolet irradiation. Rejuvenation Res 2013;16:404–413.
28. Neuman RE, Logan MA. The determination of collagen and elastin in tissues. J Biol Chem 1950;186:549–556.
29. Baumann L. Skin ageing and its treatment. J Pathol 2007;211:241–251.
30. Serafini MR, Guimaraes AG, Quintans JS, Araujo AA, Nunes PS, Quintans-Junior LJ. Natural compounds for solar photoprotection: A patent review. Expert Opin Ther Pat 20151-12.
31. Warren R, Gartstein V, Kligman AM, Montagna W, Allendorf RA, Ridder GM. Age, sunlight, and facial skin: A histologic and quantitative study. J Am Acad Dermatol 1991;25:751–760.
32. Agache PG, Monneur C, Leveque JL,De Rigal J. Mechanical properties and Young's modulus of human skin in vivo. Arch Dermatol Res 1980;269:221–232.
33. Naylor EC, Watson RE, Sherratt MJ. Molecular aspects of skin ageing. Maturitas 2011;69:249–256.
34. Kim MS, Kim YK, Cho KH, Chung JH. Regulation of type I procollagen and MMP-1 expression after single or repeated exposure to infrared radiation in human skin. Mech Ageing Dev 2006;127:875–882.
35. Song KC, Chang TS, Lee H, Kim J, Park JH, Hwang GS. Processed Panax ginseng, Sun Ginseng increases type i collagen by regulating MMP-1 and TIMP-1 expression in human dermal fibroblasts. J Ginseng Res 2012;36:61–67.
36. Chiang HM, Chen HC, Lin TJ, Shih IC, Wen KC. Michelia alba extract attenuates UVB-induced expression of matrix metalloproteinases via MAP kinase pathway in human dermal fibroblasts. Food Chem Toxicol 2012;50:4260–4269.
37. Blokhina O, Virolainen E, Fagerstedt KV. Antioxidants, oxidative damage and oxygen deprivation stress: A review. Ann Bot 2003;91:179–194.
38. Sun S, Jiang P, Su W, Xiang Y, Li J, Zeng L, Yang S. Wild chrysanthemum extract prevents UVB radiation-induced acute cell death and photoaging. Cytotechnology 2014; Jul 23. [Epub ahead of print]

39. Fisher GJ, Datta SC, Talwar HS, Wang ZQ, Varani J, Kang S,Voorhees JJ. Molecular basis of sun-induced premature skin ageing and retinoid antagonism. Nature 1996;379: 335–339.
40. Yamamoto Y, Gaynor RB. Therapeutic potential of inhibition of the NF-kappaB pathway in the treatment of inflammation and cancer. J Clin Invest 2001;107:135–142.
41. Braga PC, Dal Sasso M, Culici M, Bianchi T, Bordoni L, Marabini L. Anti-inflammatory activity of thymol: Inhibitory effect on the release of human neutrophil elastase. Pharmacology 2006;77:130–136.
42. Juergens UR, Engelen T, Racke K, Stober M, Gillissen A,Vetter H. Inhibitory activity of 1,8-cineol (eucalyptol) on cytokine production in cultured human lymphocytes and monocytes. Pulm Pharmacol Ther 2004;17:281–287.
43. Wen KC, Chiu HH, Fan PC, Chen CW, Wu SM, Chang JH, Chiang HM. Antioxidant activity of *Ixora parviflora in* a cell/cell-free system and in UV-exposed human fibroblasts. Molecules 2011;16:5735–5752.
44. Hwang YP, Oh KN, Yun HJ, Jeong HG. The flavonoids apigenin and luteolin suppress ultraviolet A-induced matrix metalloproteinase-1 expression via MAPKs and AP-1-dependent signaling in HaCaT cells. J Dermatol Sci 2011;61: 23–31.

Address correspondence to:
Janis Ya-Xian Zhan
School of Chinese Materia Medica
Guangzhou University of Chinese Medicine
Guangzhou Higher Education Mega Center
232 Wai Huan Dong Road
Guangzhou 510006
People's Republic of China

E-mail: zyx@gzucm.edu.cn

Or

Xiao-Ping Lai
School of Chinese Materia Medica
Guangzhou University of Chinese Medicine
Guangzhou Higher Education Mega Center
232 Wai Huan Dong Road
Guangzhou 510006
People's Republic of China

E-mail: lxp88@gzucm.edu.cn

Received: December 10, 2014
Accepted: April 4, 2015